Energetics and electronic structure of graphene adsorbed on HfO_2(111): Density functional theory calculations

Katsumasa Kamiya,[1,2,*] Naoto Umezawa,[3] and Susumu Okada[1,2]

[1]*Graduate School of Pure and Applied Sciences, University of Tsukuba, 1-1-1 Tennodai, Tsukuba, Ibaraki 305-8571, Japan*

[2]*Japan Science and Technology Agency, CREST, 5 Sanbancho, Chiyoda ku, Tokyo 102-0075, Japan*

[3]*Photocatalytic Materials Center, National Institute for Materials Science, 1-2-1 Sengen, Tsukuba, Ibaraki 305-0047, Japan*

(Received 16 February 2011; published 21 April 2011)

We report total-energy electronic-structure calculations based on density functional theory performed on graphene adsorbed on the (111) surface of hafnium dioxide (HfO_2). We find that the graphene is bound to the HfO_2 surface with an interlayer spacing of 3.05 Å with a binding energy of about −110 meV per C atom. The electronic structure of the HfO_2-adsorbed graphene originates primarily from that of the graphene near the Fermi level. However, a detailed analysis of the electronic structure shows that the linear bands on the Dirac cone are slightly split because of the interaction between the graphene and the HfO_2 substrate. The physical origin of this splitting is the hybridization between the π states of the graphene and the O $2p$ state with Hf d character.

DOI: 10.1103/PhysRevB.83.153413 PACS number(s): 73.22.Pr

Graphene is a carbon allotrope that is a honeycomb atomic network planar sheet. There has been a wealth of theoretical and experimental studies of the physical properties of graphene since its successful synthesis.[1] Graphene is a peculiar metal with a zero density of states at the Fermi level. This is because of the emergence of two linear dispersion bands. These linear dispersion bands lead to massless electrons near the Fermi energy, which allows for a wealth of intriguing physics. For instance, graphene has an unusually low-energy electronic structure that has remarkable transport properties, a few hundred thousand $cm^2\ V^{-1}\ s^{-1}$. Thus, graphene has the great potential to advance both the low-dimensional sciences and the next generation of nanoscale electronic devices. Recently, the integration of the graphene with a scalable gate dielectric, such as high permittivity (high-k) materials, has been the subject of a great deal of research with the goal of the realization of graphene-based electronic devices.[2–7] For the fabrication of the graphene on insulating substrates, a detailed understanding of its interactions with the substrates is critical, because they could directly affect the intrinsic electronic properties of the graphene.[8–11] In fact, the mobility of the graphene on HfO_2 is lower than that on SiO_2 and other substrates. More complexity arises from the fact that the carrier mobility is strongly affected by the HfO_2 overlayer in comparison with the SiO_2 substrate, which has been shown in a very recent study on double-oxide HfO_2/graphene/SiO_2 structures.[5] However, its underlying characteristics of the interaction are still far from being explained.

In this Brief Report, we investigate the energetics, geometry, and electronic structure of graphene adsorbed on (111) surfaces of cubic hafnia using first-principles calculations in the framework of density functional theory. We found that the graphene is bound to the HfO_2 surface via interactions with an interlayer spacing of 3.05 Å. The calculated binding energy is about −110 meV per C atom. We also found that the linear bands at the Dirac point of the graphene are slightly changed by the interactions between graphene and substrate. A detailed analysis of the electronic structure shows that the physical origin of this change is ascribed to the hybridization of the π states of the graphene with the mixed states of substrate comprising of O p and Hf d states.

To simulate a hybrid structure of graphene and HfO_2, we considered an oxygen-terminated (111) surface of a cubic phase of HfO_2 possessing a triangular lattice of O atoms at the topmost layer. The surfaces were simulated using a repeated-slab model that includes five HfO_2 layers, graphene, and a 7 Å-vacuum region (Fig. 1). We imposed a commensurability condition between the graphene and the HfO_2, where a 3×3 lateral periodicity of the graphene and 2×2 lateral periodicity of the HfO_2 surface were employed, which includes the 1.5% lattice mismatch. To bring focus to the fundamental properties of graphene adsorbed on HfO_2, we chose a lateral lattice parameter for triangular lattice $a = 7.34$ Å that was optimized for isolated graphene. The oxygen-terminated (111) surfaces of HfO_2 were then fully optimized using the same lattice parameter. In the relaxed HfO_2 slab, the Hf-O distance along the (111) direction in the topmost layer is about 3% shorter than that in the third layer because of the surface relaxation. It should be noted that in a HfO_2/graphene device, the HfO_2 has amorphous structure.[5] The surfaces used here are, therefore, hypothetical in order to simulate the interaction between π state of graphene and electron states of HfO_2. All calculations were performed using density functional theory.[12,13] We used the local-density approximation (LDA) to treat the exchange-correlation interactions among the electrons.[14] Electron-ion interactions were described using ultrasoft pseudopotentials.[15] The valence wave functions were expanded in terms of a plane wave basis set with a cutoff energy of 40 Ry. $6 \times 6 \times 1$ k points in the Brillouin zone (BZ) were sampled for BZ integration of the energetics, while $9 \times 9 \times 1$ k points were used for the self-consistent electronic structure analysis to obtain the detailed band dispersion. During the geometry optimizations, all atoms were relaxed until the residual forces were less than 0.05 eV/Å. The calculations were performed using the TOKYO AB INITIO PROGRAM PACKAGE.[16]

Figure 2 shows the binding energy of graphene on (111) surfaces of cubic HfO_2 as a function of the spacing between the graphene and the topmost O atoms in the HfO_2. To investigate

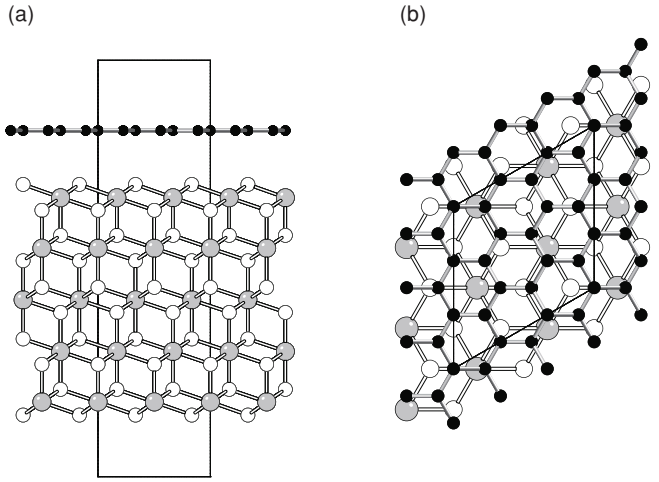

FIG. 1. (a) Side and (b) top views of the structural model. Black, gray, and white circles represent C, Hf, and O atoms, respectively. The unit cell is represented by the solid lines.

the lateral dependency of the energetics, we consider four distinct adsorption configurations of the graphene on the HfO_2. In these configurations, a C atom is located directly on the center of a Hf–O bond (Bridge), on the hollow site at the center of the Hf–O hexagonal ring (Hollow), on the top of a Hf atom (Hf top), or on the top of an O atom (O top), respectively. For all configurations, we found that the graphene is bound to the HfO_2 substrate at the optimal distance, 3.05 Å. The optimal spacing was found to be larger than the typical lengths of the C–O single or double bonds (1.42 or 1.21 Å, respectively) and the Hf–C bond in HfC (2.32 Å). This indicates that the C–O and Hf-C covalent bonds are absent in the hybrid structures. Indeed, this is consistent with the recent x-ray photoemission spectroscopy observations that there are

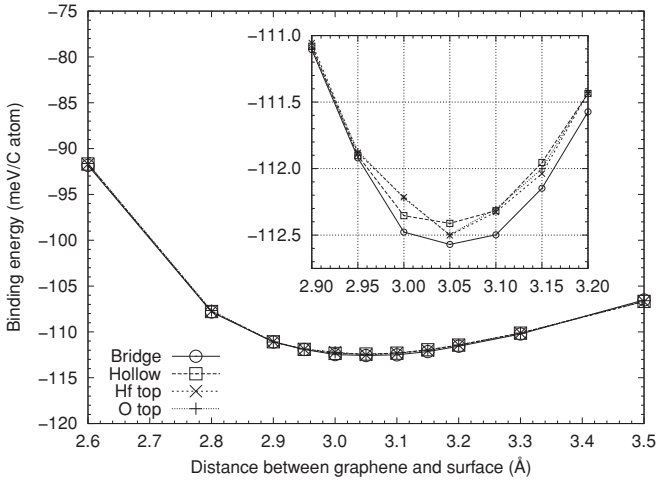

FIG. 2. Binding energy of graphene per C atom as a function of the spacing between graphene and the topmost O atoms on the HfO_2 surface for four adsorption configurations of the graphene on the HfO_2. A C atom is located directly on the center of a Hf–O bond (Bridge), on the hollow site at the center of the Hf–O hexagonal ring (Hollow), on the top of a Hf atom (Hf top), or on the top of an O atom (O top), respectively. The inset is a magnification of the area near the energy minimum.

no C–O and Hf–C bonds in HfO_2-deposited graphite[17] and HfO_2-filmed graphene on SiC substrate.[18] We also found that the value is about 6% greater than that of graphene adsorbed on O-terminated SiO_2 surfaces.[19]

At the optimum spacing, the calculated binding energy per C atom is −112 meV, irrespective of the adsorption arrangement. The specificity of the binding energy in the graphene-HfO_2 system can be understood through a comparison with the adsorption of graphene on SiO_2. Namely, the binding energy of the adsorption of graphene on HfO_2 is about eight times higher than that of graphene adsorbed on SiO_2 (Ref. 19). In the case of the graphene-SiO_2 system, it has been demonstrated that the graphene is bound to the substrate via weak van der Waals interaction.[19] By contrast, in the graphene-HfO_2 system, the present results suggest that the graphene is strongly bound to the HfO_2 surface via other mechanisms, such as orbital hybridization and electrostatic interaction, but not van der Waals interaction.

Next, we investigated the electronic structure of graphene on the HfO_2 surface. Figure 3 shows the electronic energy bands of the graphene adsorbed on the (111) surfaces of the HfO_2 with the most energetically favorable adsorption arrangement. The energy band structures of the pristine graphene and the isolated HfO_2 substrate are also shown in the same figure. In the case of the pristine graphene, both the K and K' points (Dirac point) are folded into the Γ point, because of 3×3 lateral periodicity of graphene. This results in the linear dispersion band at the Γ point. In the hybrid structure, the electronic structure seems to be a simple sum of those of each constituent. The liner dispersion bands of graphene appear in the large energy gap of HfO_2, and the energy bands associated with HfO_2 emerge as occupied and unoccupied states below −6.2 eV and above −2.8 eV (relative to vacuum level). Focusing on the linear dispersion band at the Fermi level, we found a small but significant change in these bands. From the inset in Fig. 3, it can be seen that the liner dispersion bands, which were originally degenerated at the Dirac point, are split into four branches that form a tiny fundamental energy gap of 10 meV. These results clearly indicate that the interactions between graphene and HfO_2 affect the electronic properties of graphene.

Therefore, it is worthwhile to investigate the detailed electronic properties of graphene on HfO_2 near the Fermi level. Figure 4 shows the distribution of wave functions at the Γ point for graphene on HfO_2 surface. It can be seen that the four branches of the liner dispersion states of graphene (the α, β, γ, and δ states in Fig. 4) have a hybrid nature that has properties of not only the π state of C, but also the $5d$ state of Hf and the $2p$ state of O. Indeed, these states are primarily distributed on the C atomic site with π-state characteristics. However, they also have a finite amplitude on the atomic sites on the topmost and the second subsurfaces of HfO_2. Furthermore, the bonding characters in the π-d hybridization can be seen in the wave-function distribution of the α and β states, which is shown in Fig. 4. This phenomenon is ascribed to the surface relaxation of HfO_2 substrate, which increases the covalent character of the surface HfO_2 atoms with decreasing their original ionic character. As a result of the relaxation, the high-lying valence states of the HfO_2 substrate have both $2p$ of O and $5d$ of Hf characters that originates from the topmost

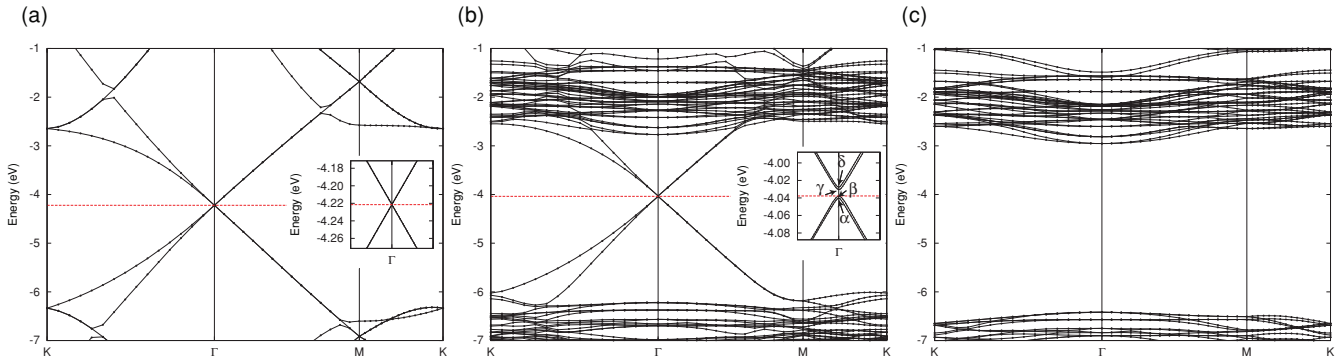

FIG. 3. (Color online) Electronic structures of the (a) isolated graphene, (b) HfO_2-adsorbed graphene, and (c) isolated HfO_2 substrate. Energies are measured from the vacuum levels, which are evaluated from the values of the self-consistent local potential at the edge of the unit cell. The horizontal red lines in panels (a) and (b) show the position of the Fermi level. In panel (c), the energy bands located below −6.5 eV are occupied, while those above −3 eV are unoccupied. The insets in panels (a) and (b) are a magnification of the area near the linear dispersion band at the Γ point. The labels α–δ refer to the states shown in Fig. 4.

HfO_2 atoms. This valence bands can then hybridize with π states of graphene.

The orbital hybridization between graphene and HfO_2 substrate is also considered to be an essential mechanism for the suppression of carrier mobility in graphene adsorbed on HfO_2 in metal-oxide-semiconductor field-effect transistor devices. Especially, because the *d* state of Hf atoms are tightly localized around the atomic sites, they may act as scatterers for the π electrons on graphene. The distribution of the wave functions near the Fermi level in the graphene-HfO_2 system corroborates our assertion that π electron states of graphene are affected by the orbital hybridization. To estimate the magnitude of the effect of the hybridization on the mobility suppression on graphene on a HfO_2 substrate, we calculated the projection of the wave function onto that of an isolated graphene sheet. The calculation provides a rough estimation of the transmission coefficient, T, for π electrons on graphene adsorbed on HfO_2:

$$T \propto |\langle \psi_G | V | \psi_G \rangle|^2,$$

where ψ_G are the π electron wave function of an free-standing graphene sheet and V is an impurity potential ascribed to the HfO_2 substrate. The calculated transmission coefficient of graphene on HfO_2 was about 70% as compared with that of the isolated graphene. This directly implies lowering the electron mobility in graphene since it is proportional to the transmission coefficient. Thus, our calculation qualitatively shows that the orbital hybridization between graphene and HfO_2 substrate significantly affects the carrier mobility of graphene.

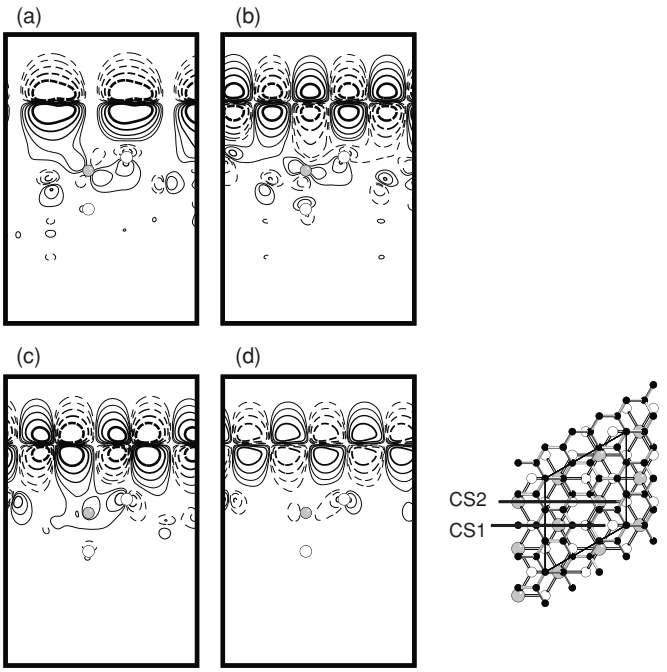

FIG. 4. Contour maps of the (a) α, (b) β, (c) γ, and (d) δ states near the Fermi level at the Γ point in graphene adsorbed on HfO_2. Each contour denotes twice (or half) the values of the adjacent contour lines from ± 0.128 $(e/\text{Å}^3)^{1/2}$. The solid and dotted lines show the positive and negative values, respectively. The two O atoms and one Hf atom that define a cross section are shown by white and gray circles, respectively. The inset in the lower right represents the position of the cross section (CS) in each figure; CS1 corresponds to panels (a) and (d), and CS2 corresponds to panels (b) and (c).

Another possible origin for the suppression of the mobility is charge depression for the π electrons on graphene. The orbital hybridization between graphene and HfO_2 results in accumulation in the spacious region between the graphene and the HfO_2 substrate. Figure 5 shows the redistribution of the valence charge after the adsorption of the graphene onto the (111) surfaces of HfO_2 with the optimal interlayer spacing. A significant charge accumulation is observed in the interlayer region, whereas an asymmetric depression is present near the graphene. This indicates that electrons are redistributed from the π states of the graphene to the interlayer spacing. Indeed, the integrated value of the density difference around the C atoms at the van der Waals distance for C (1.70 Å) is -0.001 e^- per C atom. These results suggest that the orbital hybridization between the graphene and the HfO_2 substrate changes the carrier mobility with decreasing the carrier density of π electrons in the HfO_2-adsorbed graphene.

In conclusion, we have investigated the energetics, geometry, and electronic structure of graphene adsorbed on (111)

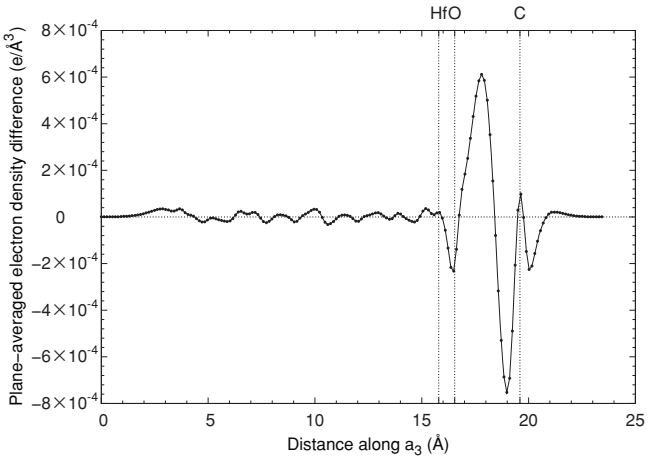

FIG. 5. Valence charge difference between the electron density of the HfO_2-adsorbed graphene and the sum of those of each component; that is, $\Delta\rho = \rho^{\text{Graphene-HfO}_2} - \rho^{\text{Graphene}} - \rho^{\text{HfO}_2}$. The values are averaged over each plane parallel to the HfO_2 surface. The vertical dotted lines indicate the positions of the C atoms in graphene and the O and Hf atoms in the first and second layers of the substrate, respectively.

surfaces of HfO_2 using total-energy electronic-structure calculations based on density functional theory. Our calculations showed that the graphene binds to the HfO_2 surface with an interlayer spacing of 3.05 Å and with a binding energy of about −110 meV per C atom. The electronic structure of the HfO_2-adsorbed graphene primarily originates from that of the graphene near the Fermi level. However, the linear bands on the Dirac cone are split because of the interaction between the graphene and the HfO_2 substrate. A detailed analysis of the wave functions revealed that the physical origin of this splitting is the hybridization of the π states of the graphene with the mixed valence states consisting of the Hf d and O p states. This study clarified a fundamental aspect of the interactions between graphene and high-k dielectric materials and provides new insight into the behavior of two-dimensional electron systems in graphene. Furthermore, this is critical for optimizing the performance of graphene-field-effect transistors fabricated with high-k materials.

Computations were performed on a NEC SX-9 at the Institute for Solid-State Physics, The University of Tokyo; a Fujitsu PrimeQuest at the Research Center for Computational Science, Okazaki Research Facilities, National Institutes of Natural Sciences; a NEC SX-8/4B at the University of Tsukuba; and a NEC SX-9 at the Information Synergy Center, Tohoku University. This research was supported by a Grant-in-Aid for Young Scientists (B) (Grant No. 22740259), in part by CREST, the Japan Science and Technology Agency, and a Grant-in-Aid for Scientific Research from the Ministry of Education, Culture, Sports, Science, and Technology of Japan.

*kkamiya@comas.frsc.tsukuba.ac.jp

[1] K. S. Novoselov, A. K. Geim, S. V. Morozov, D. Jiang, Y. Zhang, S. V. Dubonos, I. V. Grigorieva, and A. A. Firsov, Science **306**, 666 (2004).
[2] I. Meric, M. Y. Han, A. F. Young, B. Ozyilmaz, P. Kim, and K. L. Shepard, Nat. Nanotechnol. **3**, 654 (2008).
[3] J. Kedzierski, P.-L. Hsu, P. Healey, P. W. Wyatt, C. L. Keast, M. Sprinkle, C. Berger, and W. A. de Heer, IEEE Trans. Electron. Devices **55**, 2078 (2008).
[4] J. A. Robinson, M. LaBella, K. A. Trumbull, X. Weng, R. Cavelero, T. Daniels, Z. Hughes, M. Hollander, M. Fanton, and D. Snyder, ACS Nano **4**, 2667 (2010).
[5] K. Zou, X. Hong, D. Keefer, and J. Zhu, Phys. Rev. Lett. **105**, 126601 (2010).
[6] L. Liao, J. Bai, Y. Qu, Y.-c. Lin, Y. Li, Y. Huang, and X. Duan, Proc. Natl. Acad. Sci. USA **107**, 6711 (2010).
[7] L. Liao, J. Bai, R. Cheng, Y.-C. Lin, S. Jiang, Y. Huang, and X. Duan, Nano Lett. **10**, 1917 (2010).
[8] S. Y. Zhou, G.-H. Gweon, A. V. Fedorov, P. N. First, W. A. de Heer, D.-H. Lee, F. Guinea, A. H. Castro Neto, and A. Lanzara, Nat. Mater. **6**, 770 (2007).
[9] A. Mattausch and O. Pankratov, Phys. Rev. Lett. **99**, 076802 (2007).
[10] S. Fratini and F. Guinea, Phys. Rev. B **77**, 195415 (2008).
[11] L. A. Ponomarenko, R. Yang, T. M. Mohiuddin, M. I. Katsnelson, K. S. Novoselov, S. V. Morozov, A. A. Zhukov, F. Schedin, E. W. Hill, and A. K. Geim, Phys. Rev. Lett. **102**, 206603 (2009).
[12] P. Hohenberg and W. Kohn, Phys. Rev. **136**, B864 (1964).
[13] W. Kohn and L. J. Sham, Phys. Rev. **140**, A1133 (1965).
[14] J. P. Perdew and A. Zunger, Phys. Rev. B **23**, 5048 (1981).
[15] D. Vanderbilt, Phys. Rev. B **41**, 7892 (1990).
[16] J. Yamauchi, M. Tsukada, S. Watanabe, and O. Sugino, Phys. Rev. B **54**, 5586 (1996).
[17] A. Pirkle, R. M. Wallace, and L. Colombo, Appl. Phys. Lett. **95**, 133106 (2009).
[18] Q. Chen, H. Huang, W. Chen, A. T. S. Wee, Y. P. Feng, J. W. Chai, Z. Zhang, J. S. Pan, and S. J. Wang, Appl. Phys. Lett. **96**, 072111 (2010).
[19] N. T. Cuong, M. Otani, and S. Okada, Phys. Rev. Lett. **106**, 106801 (2011).